ELSEVIER

NeuroImage

www.elsevier.com/locate/ynimg
NeuroImage 37 (2007) 1237–1249

A novel approach to clinical–radiological correlations: Anatomo-Clinical Overlapping Maps (AnaCOM): Method and validation

Serge Kinkingnéhun,[a,b,c,*] Emmanuelle Volle,[a,d,e,f] Mélanie Pélégrini-Issac,[b,j] Jean-Louis Golmard,[g] Stéphane Lehéricy,[a,b,e,f,h] Foucaud du Boisguéheneuc,[a] Sandy Zhang-Nunes,[a,i,n] Danielle Sosson,[k] Hugues Duffau,[b,j,l] Yves Samson,[a,m] Richard Levy,[a,d,f,k] and Bruno Dubois[a,d,f,k]

[a]*INSERM U610, Paris, France*
[b]*IFR-49, SHFJ, Orsay, France*
[c]*e(ye)BRAIN, Paris, France*
[d]*IFR-70, Paris 75013, France*
[e]*Service de Neuroradiologie, Groupe Hospitalier Pitié-Salpêtrière, Paris, France*
[f]*Université Pierre et Marie Curie-Paris6, Paris, France*
[g]*INSERM Unité Fonctionnelle de Biostatistique et Informatique Médicale, Paris 75013, France*
[h]*Center for NeuroImaging Research – CENIR, Paris, France*
[i]*Department of Brain and Cognitive Sciences, Massachusetts Institute of Technology, MA, USA*
[j]*INSERM U678, Paris, France*
[k]*Fédération de Neurologie, Groupe Hospitalier Pitié-Salpêtrière, Paris, France*
[l]*Neurochirurgie, AP-HP, Hôpital de la Salpêtrière, Paris, France*
[m]*Urgences cérébro-vasculaire, Groupe Hospitalier Pitié-Salpêtrière, Paris, France*
[n]*Johns Hopkins University School of Medicine, Baltimore, MD, USA*

Received 18 December 2006; revised 4 June 2007; accepted 25 June 2007
Available online 12 July 2007

We present a new clinical–radiological correlation method (AnaCOM) that aims at establishing structure–function relationships. We validated AnaCOM by assessing the location of lesions that are associated with altered performances in a well-studied task: the verbal fluency task. We retrospectively reviewed 64 brain-damaged patients who had focal lesions in a variety of cortical sites due to stroke, hemorrhage or tumor surgery. All patients were tested for verbal fluency at the time of the MRI examination. MRI volumes were normalized using a mask covering brain lesions and artifacts. The brain lesions were then segmented using the normalized MRI. In each patient, a verbal fluency score was assigned to each voxel in the segmented area. Subsequently, segmentations were superimposed and voxels were gathered in clusters defined by the overlap of the patients' lesion. For each cluster, the scores were statistically compared to those obtained by controls for the same task. This process allowed the construction of cluster-by-cluster statistical maps of anatomo-clinical correlations. As expected, the statistical map indicated that two regions were significantly associated with a deficit in the fluency task: one located in Broca's area and the other in the preSMA. AnaCOM does not require a priori selection of the location of lesions or task scores. The method complements the functional imaging techniques, as it tells which regions are necessary for a given function and it explores cortical regions as well as the white matter.

Keywords: AnaCOM; Anatomo-Clinical Overlapping Map; Anatomical MRI; Neuropsychological test; Verbal fluency; Brain lesion

Introduction

Paul Broca made a great contribution to the study of the brain by introducing the concept of localization of functions to different regions of the brain. He postulated that the brain damage of the patient "Tan", who suffered from aphasia, was precisely located in the area which controls speech. By studying the brain damage of aphasic patients after their death, Broca demonstrated that there was a relatively circumscribed center located in the posterior and inferior convolutions of the left frontal lobe, now known as "Broca's area," that was responsible for speech (langage articulé) (Broca, 1861a,b,c,d, 1863, 1865). These pioneering studies estab-

* Corresponding author. INSERM U610, Pavillon Claude Bernard, Groupe Hospitalier Pitié-Salpêtrière, 47-83 boulevard de l'Hôpital, 75013 Paris, France. Fax: +33 1 42 16 41 95.
E-mail address: serge@skinkin.com (S. Kinkingnéhun).
Available online on ScienceDirect (www.sciencedirect.com).

1053-8119/$ - see front matter © 2007 Elsevier Inc. All rights reserved.
doi:10.1016/j.neuroimage.2007.06.027

lished the clinico-pathological correlation technique, which consists of relating a functional deficit to a specific brain lesion observed after the death of the patient or through the use of structural brain imaging. The clinico-pathological correlation technique has been widely used since then to correlate functional deficiencies with brain lesions both in patients and in healthy animals (Cromwell and Berridge, 1993).

With the arrival of new tools in neuroimagery that allow one to be able to "see" inside the living body, it is now easier to produce correlations between human functional deficits and brain lesions. Magnetic resonance imaging (MRI) allows for more precise observation of tissue damage in vivo. Approaches to anatomo-clinical correlations fall into one of three groups. The first group is similar to clinico-pathological correlation, but describes patient lesions, as shown by structural MRI, through case reports (Pierrot-Deseilligny et al., 1991; Rivaud et al., 1994; Gaymard et al., 1998), compilations of case reports (Kertesz, 1993), or recruitment of subjects with similar lesions (Braun et al., 1992; Regan et al., 1992; Lekwuwa and Barnes, 1996; Greenlee and Smith, 1997; Stuss et al., 1998; Beblo et al., 1999; Ayotte et al., 2000; Furst et al., 2000). This approach works well if we assume that the occurrence of a deficit depends on the lesion of a single structure (Godefroy et al., 1998).

The second type of approach can be generalized under the term "maximum overlap". Since all patients experience a similar functional deficit, the region of maximum overlap (i.e., the area most commonly damaged) is the region of voxels associated with the deficient function (Clarke et al., 1997; Lippitz et al., 1997; Tranel et al., 1997; Haaland et al., 2000; Stufflebeam et al., 2000; Makale et al., 2002; Milea et al., 2003; Parvizi and Damasio, 2003; Van der Werf et al., 2003). Maximum overlapping techniques, however, focus on a single region that is linked to a function and do not provide any information on the potential implication of other areas that may or may not be involved in a particular function.

More recently, several authors have attempted to take into account the possibility of detecting multiple areas for a function. They set up a new method inspired by both the voxel-based approach and the maximum overlap approach. These methods aim to obtain a map showing regions which are linked to a neuropsychological deficit. Another approach was to segment lesions in a normalized standardized space and to weight the voxels inside lesions either positively or negatively (Cohen et al., 2003) or with the score obtained by a patient in a neuropsychological test (Frank et al., 1997; Kinkingnéhun et al., 2004). These techniques allow one to obtain maps presenting averaged scores for each voxel. These two techniques permit one to find several sets of contiguous voxels (clusters) of the brain participating in a single function, but they are not statistical methods. To improve the effectiveness, the neuropsychological score of those who have lesions in a particular voxel can be statistically compared with those who do not have lesions in the studied voxel (Bates et al., 2003; Dronkers et al., 2004; Karnath et al., 2004a; Committeri et al., 2007). These voxel-based methods greatly improve on the classical anatomo-clinical method, as they do not require a priori selection of patients based on their scores at neuropsychological tests or selection on the basis of the location of the lesions. Statistical comparison of patients with the deficit vs. control patients without the deficit, instead of patients vs. healthy controls can be discussed. Moreover, the stringent Bonferroni correction that is applied to voxel by voxel statistical method greatly reduces the statistical power (Rorden and Karnath, 2004).

Therefore, we developed a cluster-of-voxels-based method, called the Anatomo-Clinical Overlapping Maps (AnaCOM) method, that allows for the generation of statistical anatomo-functional maps from patients with brain lesions (Kinkingnéhun et al., 2004). We also optimized the lesion segmentation and lesion normalization stages of the procedure. By rating the performance of patients on neuropsychological tests and capturing their brain structure with a structural MRI scan, we were able to develop maps that correlated a set of contiguous voxels in the brain with the degree of neuropsychological deficit when compared to the score of normal control subjects.

Application of the AnaCOM method was performed with a verbal fluency task. We chose the phonemic verbal fluency task (Cardebat et al., 1990) because it is related to a well-known and reliable cerebral network. Word generation tasks have also been used to map Broca's area in electrophysical and fMRI studies in a reliable and accurate correspondence (Brannen et al., 2001). We expected AnaCOM to show areas of the fronto-temporo-parietal network usually involved in verbal fluency tasks. A voxel-based approach, the voxel-based lesion-symptom mapping (VSLM) (Bates et al., 2003), was also performed on the same data set and in the same conditions in order to compare the results of the two methods. AnaCOM was predicted to be more sensitive than the VSLM.

Anatomo-Clinical Overlapping Maps

Overview

The aim of this method is to create anatomo-clinical maps from patients with brain lesions. These maps are created using the anatomical MRI of patients who are administered neuropsychological tests (see Fig. 1). First, MRIs are normalized to a common standardized space. Second, brain lesions are segmented to obtain regions of interest (ROI). Third, the score obtained by the patient in the neuropsychological test is introduced in the voxels of the segmented ROI. Lesions are overlapped and voxels are gathered in clusters according to the patients' brain lesions which cover them. Finally, the patient's score for each cluster is statistically compared to normal values, which allows for the creation of statistical maps.

Image acquisition

The MRI images required for AnaCOM studies are anatomical scans on which lesion boundaries are clearly visible. 3D T1 anatomical MRI allows one to see both vascular and tumor excision lesions.

Structural MRI normalization

Patient anatomical MRI scans are normalized to allow comparison. Damaged areas of the images (lesions and artifacts) are masked to reduce their influence in the normalization process (Brett et al., 2001). MRI scans are normalized to fit each patient's brain, according to the T1 Montreal Neurological Institute (MNI) Atlas (see Fig. 2).

Mask

As the registration process uses signal intensity of the voxels, artifacts and the signal generated by lesions can influence the normalization process (Ashburner et al., 1997). Thus, the signal

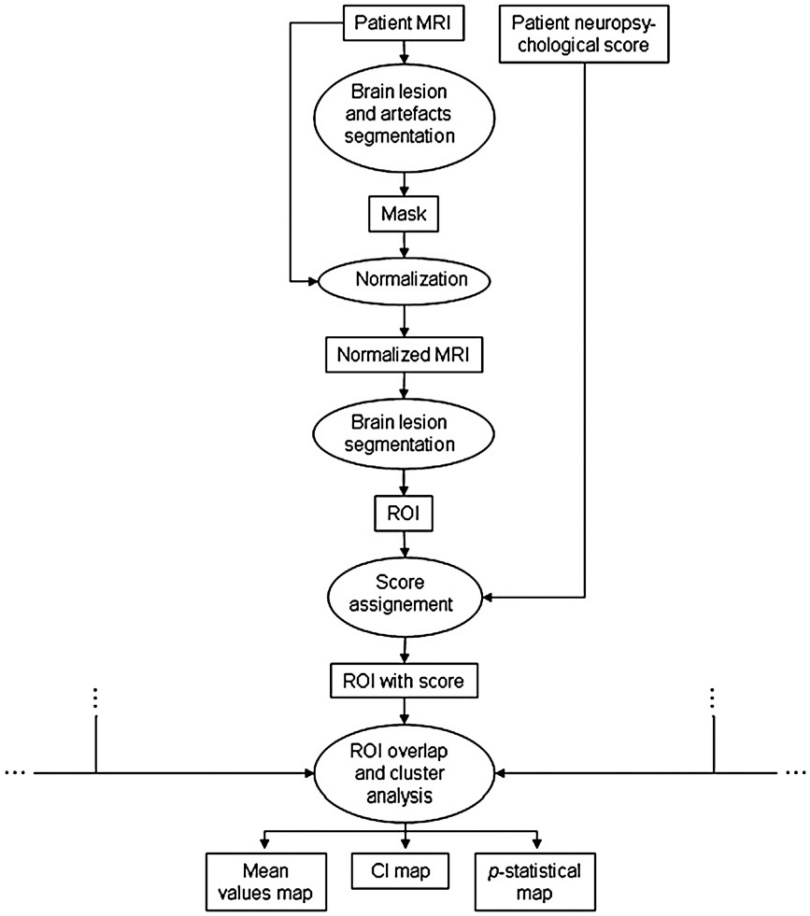

Fig. 1. General flow chart diagram of the AnaCOM process.

abnormalities are manually segmented to create binary masks to exclude signal abnormalities during normalization (Brett et al., 2001). The masks cover all signal abnormalities due to either lesions or artifacts. The masks must be larger than the actual lesions.

Normalization

Structural MRI scans of all patients are transformed to the same stereotactic space. Each scan is registered to the same template image, using the residual sum of squared differences as the matching criterion. The first step in spatial normalization involves

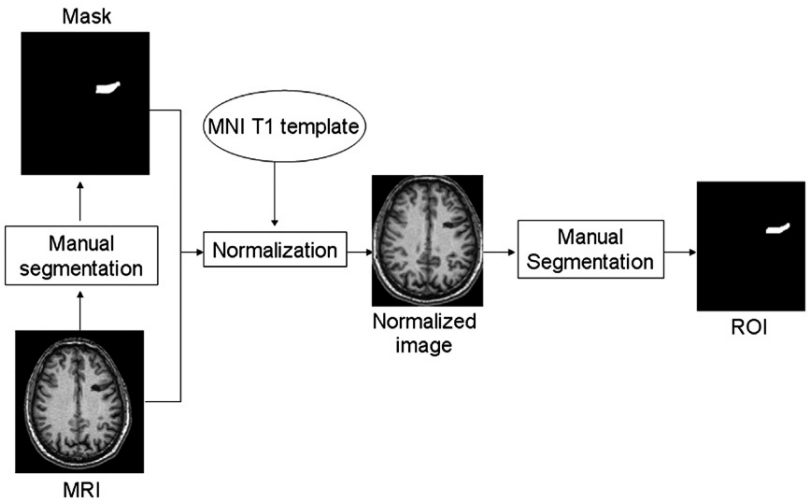

Fig. 2. Flow chart diagram showing the normalization and segmentation process.

the estimation of the optimum 12-parameter affine transformation to match images (Ashburner et al., 1997). A Bayesian framework is used, whereby the maximum a posteriori estimate of the spatial transformation is made using prior knowledge of the normal variability in brain size. The second step accounts for global non-linear shape differences, which are modeled by a linear combination of smooth spatial basis functions (Ashburner and Friston, 1999). A masking procedure is used to weight the normalization to brain, rather than non-brain tissue or lesions (Brett et al., 2001). The spatial normalized images are re-sliced with a final voxel size of $1.5 \times 1.5 \times 1.5$ mm^3. The normalized images are visually inspected to check for misregistration with the template. In our study, none of the normalized images gave unsatisfactory results.

Lesion segmentation

Brain lesions are manually segmented on the normalized anatomical MRI. This process allows better control of the delimitation of the lesion border than drawing the lesion directly on an atlas while looking at the patient lesion MRI (Mort et al., 2003; Dronkers et al., 2004; Karnath et al., 2004b), or applying the deformation matrix to the lesion mask and transforming it to a binary image. Lesion segmentation allows one to obtain a ROI image representing the lesion of a patient. For surgical resections, the ROI included the resection cavity filled with CSF. For stroke, we only considered the infarcted part of the tissues. Tissue showing signal abnormalities surrounding the resection cavity or the infarct may still be functional. Moreover, activation studies have shown that peri-infarct regions can be activated (Warburton et al., 1999; Leger et al., 2002; Butefisch et al., 2006) and are important for recovery. Thus, by being very conservative in the inclusion of voxels in the ROI image, our procedure avoids false positives, but also may underestimate lesion size.

Assignment of performance to the lesion

For consistency, a patient's segmented lesion from here on will be called an ROI image. To generate AnaCOM, the score obtained by the patient in the neuropsychological test is introduced into their ROI image (Fig. 3). Each voxel's value of the ROI is replaced by the functional score of each patient, while the rest of the image is set to zero, assuming that the brain lesion is responsible for the patient's deficit. Therefore, the 3D images are composed of two different types of voxels: voxels included in the ROI express the score value obtained by the patient at the chosen neuropsychological test and the others are set to zero.

Anatomo-clinical overlaps

Definition of a cluster of voxels

We define a cluster of voxels as a group of contiguous voxels covered by the same ROIs. In Fig. 4, the ROIs A to F are segmented normalized lesions from five different patients. Each intersection of the ROIs forms a subgroup. This subgroup, in a discrete space where the basic unit is a voxel, is called a cluster of contiguous voxels. Each voxel in a given cluster is an overlap of voxels from exactly the same ROIs (i.e., all voxels in a given cluster contain the same information) and must be contiguous, according to the 26-neighborhood topological definition, with at least one other voxel of the cluster (see Fig. 5) (Bertrand, 1994; Bertrand and Malandain, 1994). The minimum size of a cluster is a single voxel.

Maximum Overlap Map

The Maximum Overlap Map is created from the patients' ROI. All the ROI are superimposed in the normalized space. Each voxel value of the map represents the number of patients whose ROI covers the voxel. The map is thresholded to remove voxels corresponding to less than n overlaps ($n=3$). The resulting mask

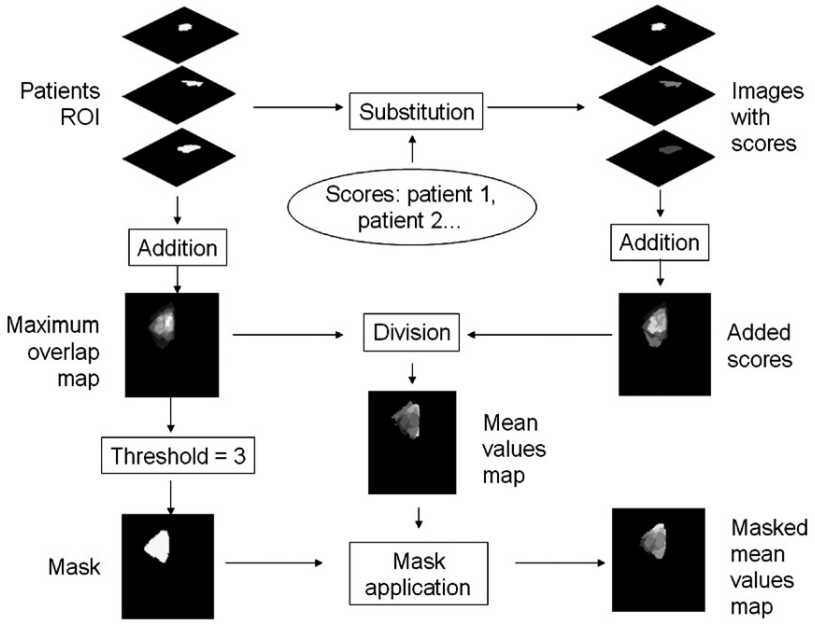

Fig. 3. Flow chart diagram showing the preprocessing steps to build up the mean value AnaCOM.

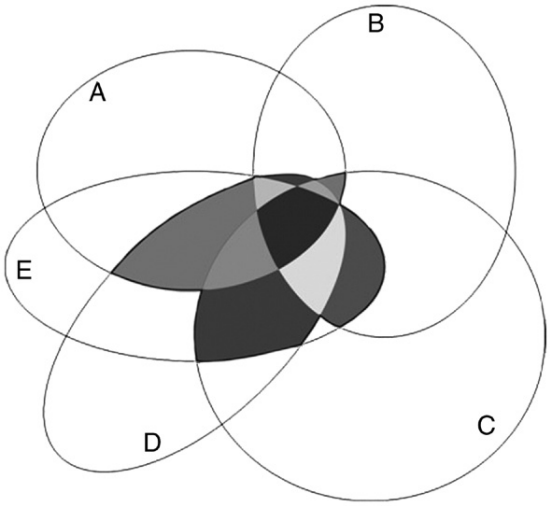

Fig. 4. ROIs overlapping and cluster definition. A to E are ROIs defined by normalized and segmented patients' lesion. The ROIs' intersections define subregions. In a discrete space, subregions are clusters of contiguous voxels. Each cluster is filled in with a different level of gray. Here, only the clusters with at least 3 overlaps are grayed.

will be used in the process to avoid statistical errors in the p-statistical map (described below) and in the Mean Value Map. The resulting thresholded map reveals the areas from which the following maps are analyzed.

Mean Value Map

The Mean Value Map is generated from the Maximum Overlap Map and the scores obtained by the subjects (see Fig. 3). The weighted ROI for all patients is superimposed, summing the values of each of their voxels. The values obtained for the voxels included in the overlap of the ROIs are divided by the number of patients having an ROI at that site. Areas having less than n overlaps are removed by thresholding because their average values would not be an adequate representation. These voxels are set to zero.

Half Length 95% Confidence Interval

The Confidence Interval Map ($CI_{95\%}$ map) is created from the weighted ROI and the patients' scores. The Half Length 95% Confidence Interval ($CI_{95\%}$) gives an estimated range of values which is likely to include an unknown population parameter. The estimated range is calculated for each voxel of the image from the score of the patient's having brain damaged in the voxel. $CI_{95\%}$ is calculated as follows:

$$CI_{95\%}(x) = \overline{x} \pm 1.96 \frac{s}{\sqrt{n}}$$

where x is the value obtained in a voxel, $\overline{x}$ is the average of the values obtained by the patients whose lesions overlap in a voxel:

$$\overline{x} = \frac{1}{n} \sum_{l=1}^{n} x_i$$

and s is the standard deviation of the test score values in the same voxel:

$$s = \sqrt{\frac{1}{n-1}\left(\sum_{l=1}^{n} x_i^2 - \frac{1}{n}\left(\sum x_i\right)^2\right)}$$

with xi the score value for a patient, n the number of patients whose lesion is overlapping in the evaluated voxel.

p-statistical map

The p-statistical map is created from the overlap of the ROI of the patients. The overlaps of the ROI define clusters. For each cluster determined by the Maximum Overlap Map (see above), the scores obtained by the patients are statistically compared to the scores of a group of normal controls or to normative values obtained for this test (see Fig. 3). Statistics produced for each cluster do not have the same number of degrees of freedom, since clusters may correspond to the overlap of different numbers of patients. Thus, the map displays the p-value rather than the statistical score itself (t-score) to avoid biases due to differences in the degrees of freedom when comparing clusters. Different statistics can be applied depending on whether the scores of the controls follow a normal distribution (Student's t-test) or not (Kolmogorov–Smirnov test or Wilcoxon test) (see Fig. 6).

Interpretation of the results

The Maximum Overlap Map shows the clusters included in the analysis. The Mean Value Map presents a picture of the clusters involved in the perturbation of the neuropsychological score. The $CI_{95\%}$ map gives an indication of the precision of the mean score values of the Mean Value Map. The p-statistical map shows the p-values for the statistical test when scores of healthy control subjects are normally distributed. Otherwise, non-parametric tests such as the Kolmogorov–Smirnoff test or the Wilcoxon test are

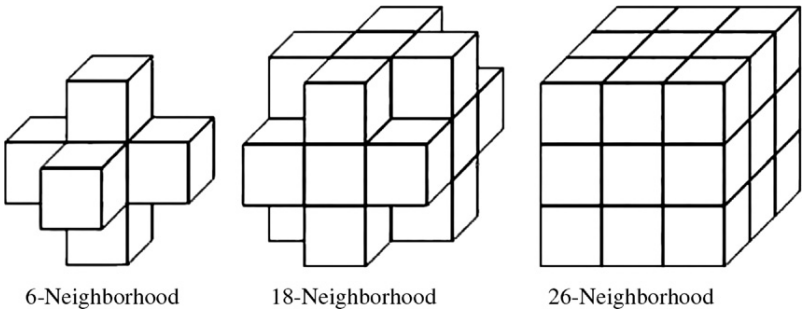

Fig. 5. Topological voxel neighborhood. The 3 illustrations show the voxels contiguous to the central voxel in a 6-, 18- and 26-neighborhood. In our definition of clusters, voxels are contiguous in a 26-neighborhood.

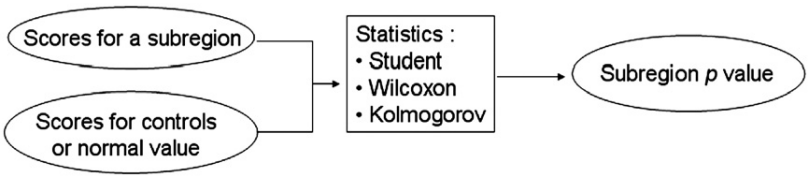

Fig. 6. Flow chart diagram showing the *p*-value calculation for a cluster. For each cluster, a *p*-value is evaluated using the scores of the subjects having a lesion within the cluster compared to either a normal value or the scores obtained by normal control subjects.

used, comparing the vector of score values of the "brain lesion" group to the one of the control group for each cluster. Maps are Bonferroni-corrected depending on the number of clusters compared (see Figs. 7 and 9).

Thus, clusters can be examined on one hand, by both their mean value and $CI_{95\%}$ and, on the other hand, by their *p*-value (Fig. 9). By comparing the performance of controls and patients on particular neuropsychological tasks using these maps, one can identify areas that are likely to contribute to the function needed for normal performance on the task. The results can only be interpreted reliably, however, for an overlap of a minimum of three lesions.

Validation

Material used for processing

We developed the AnaCOM method in the Python language using BrainVISA software (Institut Fédératif de Recherche IFR-49, Orsay, France, http://www.brainvisa.info/). We used modules from AIMS and VIP Libraries (SHFJ-CEA, ORSAY, France, http://www.brainvisa.info/) (Cointepas et al., 2001) provided by BrainVISA, and SPM2 (Wellcome Department of Imaging Neuroscience, Institute of Neurology, London, UK, http://www.fil.ion.icl.ac.uk/spm) (Friston, 1995) in conjunction with MATLAB version 6.5 (The Mathworks, Inc., MA, USA) to create a whole data processing pipeline. All the statistics were computed with the R library (http://www.r-project.org/) (Ihaka and Gentleman, 1996). The pipeline will be distributed with BrainVISA as a plug-in. Display of 3D images was done with Anatomist (SHFJ-CEA, ORSAY, France, http://www.brainvisa.info/) (Rivière et al., 2000). The manual segmentations of the lesions and artifacts of the images of the patients were performed with MRIcro (http://www.mricro.com). The VSLM analysis was performed with NPM (http://www.sph.sc.edu/comd/rorden/mricron/tutorial/index.html).

Populations used for validation

For this study, we retrospectively reviewed 64 brain-damaged patients (see demographic data in Table 1) who had lesions in a variety of cortical sites due to various etiologies (e.g., stroke, hemorrhage, tumor excision). The criteria for inclusion in the study were the following: patients had (1) focal brain lesions shown in a T1 weighted 3D MRI scan, and (2) had performed the phonemic verbal fluency task. Patients included in the study underwent MRI scans and the neuropsychological examinations within 1 month of the onset of their brain damage. The neuropsychological profile did not influence patient selection. All patients were right-handed, ranging in age from 23 to 72 (mean ± SD = 46.77 ± 10.26). They were recruited from the neuropsychological, the neurosurgery departments and the stroke center of the Pitié-Salpêtrière Hospital. We voluntarily included patients with different mechanisms of brain damage (tumor surgery, stroke and hemorrhage). Mixing lesions of various origins avoided artifacts of coincident association between (1) one specific region and one cause (for example stroke) and (2) one specific deficit from one cause.

All patients were administered the phonemic verbal fluency task (Cardebat et al., 1990) in a standardized manner by a psychologist, at the Neuropsychological and language center of the Salpêtrière Hospital. Patients were asked to verbally generate as many words as possible beginning with the letter "M". Answers were handwritten by the examiner and counted. The number of words given in one minute constituted the score used for the analysis. The performances of patients were compared to the normative value established in 20 control subjects matched for age (40 to 60 years old) and educational level (all controls were at level 5). Control subjects did not present with brain lesions or known neuropsychological disease. All subjects signed informed consent.

Image acquisition

A 1.5-T MR General Electric scanner was used to perform all image acquisition. Inversion Recovery SPGR T1-weighted images (TE = 2.02; TR = 10.1; inversion time = 600 ms; pixel bandwidth = 97.66; flip angle = 10°; acquisition matrix = 256 × 192; field of view = 240 × 180 mm^2; slice thickness = 1.5 mm; pixel size = 0.9375 mm × 0.9375 mm) were acquired in the orthogonal plane.

AnaCOM maps

We analyzed voxel clusters of the brain which were covered by at least three lesions. We weighted each ROI by the score obtained by each patient in the verbal fluency task. The scores of the control subjects followed a normal distribution. Therefore, we used a one

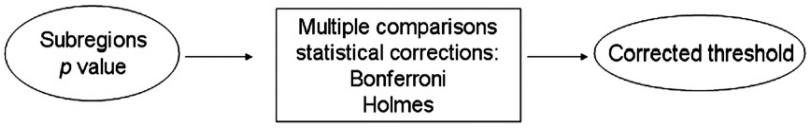

Fig. 7. Flow chart diagram showing the correction for multiple comparisons of the clusters' *p*-value. A threshold correcting for multiple comparisons is calculated from the *p*-values of the map.

Table 1
Demographic and descriptive data

Patients	$n=64$	Mean	Standard deviation	Minimum	Maximum
Age		47.6	10.9	26	72
Educational level [a]		5.4	1.5	2	7
Lesion volume [b]		42.4	44.2	0.8	192.2
Interval [c]		18.3	16.8	1	75
		n	%		
Gender	Male	41	64.1		
	Female	23	35.9		
Lesion side	Right	28	43.8		
	Left	35	54.7		
	Bilateral	1	1.5		
Etiology	Vascular	33	51.6		
	Surgery	31	48.4		

[a] Educational level from the Barbizet score, quotation from 1 to 7.
[b] Volume of the lesions in cm^3.
[c] Interval in months, between the vascular lesion onset or the tumour surgery and the task performance.

sample Student's *t*-test for statistical comparisons (i.e., we compared the patients' scores to the mean score obtained by the 20 normal controls). The resulting *p*-statistical map can be seen in Figs. 9 and 10.

VSLM analysis

The VSLM analysis was performed on the same set of patients as the AnaCOM method (e.g., with the same ROIs and the same scores obtained for fluency) in the same conditions: a *t*-test, without permutations, testing voxels damaged in at least 3 individuals while using the Bonferonni FWE *Z* threshold. The only difference lies in which two samples the comparison was performed. VSLM compares patients having brain damaged for the tested voxels vs. patients not damaged for those voxels while AnaCOM compares patients having brain damage vs. normal controls.

Results

Fig. 8 shows the overall locations of the lesions. The red area corresponds to the voxels in which at least three lesions overlapped. This map covered a large part of the brain bilaterally. In the left hemisphere, almost the entire frontal lobe was included, as well as the insula, the cingulum, the superior temporal gyrus, the temporal pole, the inferior parietal lobule, the supramarginal and the angular gyrus. In the right hemisphere, the superior, middle and inferior frontal gyri were included, as well as the postcentral and supramarginal gyrus, and the superior, middle and inferior temporal gyri. The mean value of these clusters (Fig. 9) extended from 0.33 (in red) to 17.75 (in yellow). The clusters in which the mean value was the lowest were the left perisylvian area, the insula, the inferior frontal gyrus, the superior temporal gyrus and the temporo-parietal area.

The statistical map (Bonferroni-corrected) indicated two sets of clusters that were significantly associated with a deficit in the fluency task (Figs. 9 and 10; Table 2): (1) the posterior portion of the inferior frontal sulcus, in the triangular part, next to the vertical ramus of the lateral sulcus. This area belonged to Broca's area; (2) the anterior part of the supplementary motor area (SMA), described previously as the preSMA and the adjacent medial superior frontal gyrus.

Besides the validation aspect, we looked at a lower threshold to check for the tendencies of our results. Using a lower threshold ($p<0.001$ uncorrected), to examine the mean value and CI maps, other left-sided areas seemed also to be important for the phonemic

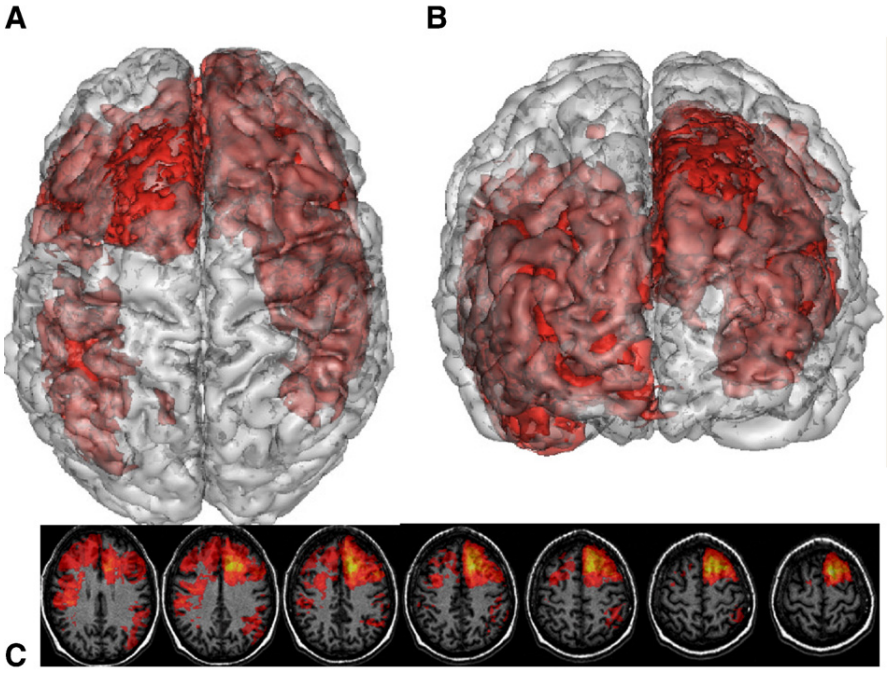

Fig. 8. (A) Superior and (B) anterior views of the areas of the brain covered by at least 3 overlaps of patients' lesions. (C) Axial sections showing the number of overlaps (from 3 overlaps in dark red, to 11 overlaps in bright yellow).

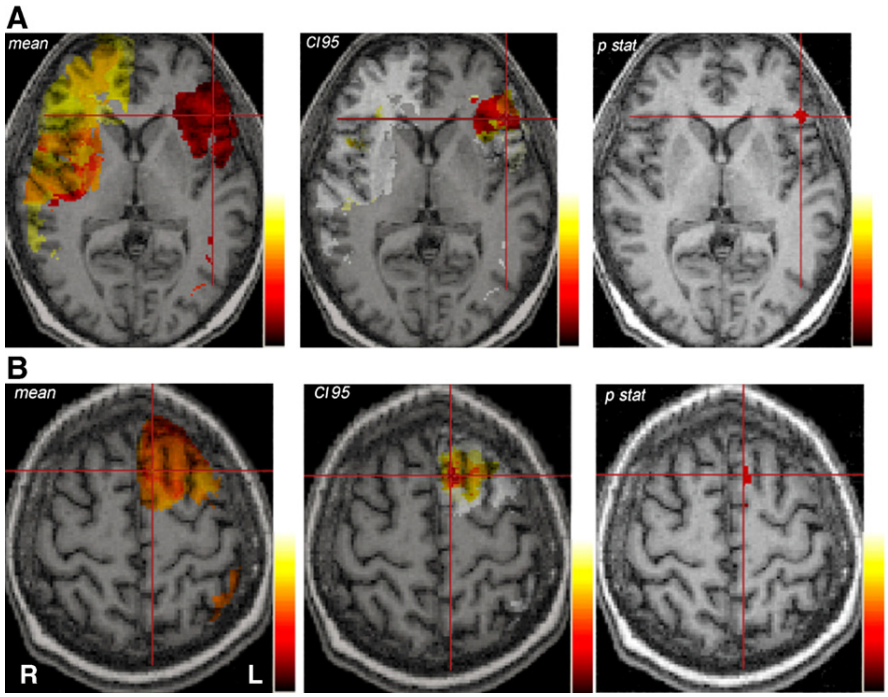

Fig. 9. Mean value, 95% CI and *p*-statistical maps showing the implication of the (A) Broca area and (B) preSMA in the fluency task. The mean values (range value from 0.33 in red to 17.75 in yellow) and 95% CI (range value from 0.32 in red to 2 in yellow). In white are shown regions with CI value superior to 2, in order to show the information for all the studied clusters. The *p*-statistical map is thresholded with a Bonferroni correction (range value from 0 in red to 2.8×10^{-5} in yellow).

fluency task. These are listed in Table 2: the left anterior insula, the operculum and orbital part of the inferior frontal gyrus, including the surrounding white matter, the inferior frontal sulcus and the cingular cortex. All these areas show clusters with a low mean score value and a small $CI_{95\%}$ as compared to the mean map and the $CI_{95\%}$ map, which attest to their implication in the deficits of the patients.

All areas on the right, including those showing a low mean value, had a large $CI_{95\%}$ value and a *p*-value >0.001.

Regarding the VSLM analysis, VSLM tested 349,454 voxels whereas AnaCOM compared 1642 clusters. This drastically reduced the Bonferroni correction: no voxels could be found with a Bonferroni correction using VSLM.

Discussion

Methodological considerations

This study shows our ability to construct anatomo-functional maps based on the structural MRI scans of patients with brain lesions using neuropsychological tests, without *a priori* knowledge of the damaged structures.

Thus, this new method allows us to go beyond the classical group methodology in studying lesions, to find brain regions more and less relevant to a deficit.

In contrast to the preceding statistical methods (Bates et al., 2003; Dronkers et al., 2004; Karnath et al., 2004a; Committeri et

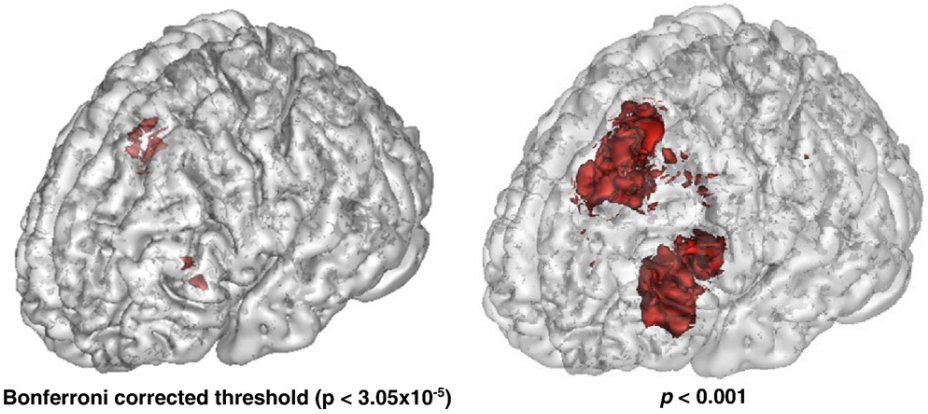

Fig. 10. *p*-statistical map thresholded with a Bonferroni correction and at $p<0.001$ uncorrected.

Table 2
Anatomical regions identified by AnaCOM to be significantly associated with a deficit in the verbal fluency task

Anatomical regions	Brodmann areas	*p*-values	Mean value	IC95
Left IFG (pars triangularis) [a]	44, 45	2.7×10^{-5}	2.5	0.58
Left preSMA [a]	6/8	3.5×10^{-6}	7.2	0.32
Left anterior insula [b]	–	8×10^{-4}	1.5	1.50
Frontal operculum [b]	6	2.5×10^{-4}	2.8	0.64
Left IFG (pars opercularis) [b]	47	2.7×10^{-4}	2.4	0.58
Inferior frontal White matter	–	8×10^{-4}	1.5	0.50
IFS	45	8×10^{-4}	1.5	0.50
Cingular cortex	24/32	1.7×10^{-4}	7.9	1.03

IFG: inferior frontal gyrus; SMA: supplementary motor area; IFS: inferior frontal sulcus.
[a] Significant at a Bonferroni-corrected threshold.
[b] Found at a 0.001 uncorrected threshold.

al., 2007) and that used by Rorden and Karnath (2004), the control group consisted of healthy subjects instead of patients with brain lesions. The previous methods could miss statistical areas linked to the deficit of a function: if a specific structure is the anatomical basis of a function, and also, if two subjects have lesion damage in a structure but not in overlapping areas, then the statistical comparison in the structure would have lower statistical power (see Fig. 11). This problem was avoided in our study by comparing subjects with a lesion covering a particular cluster of voxels with normal subjects having no lesion at all. Rorden and Karnath (2004) state that the control group should be composed of patients with brain lesions and must be similar to the patients of interest with respect to other variables, such as other neuropsychological symptoms. This method of design probably aimed to avoid comparing populations which are too different from each other, but in our method, such population differences could be accounted for using ANCOVAs.

Previous lesion studies (Bates et al., 2003; Dronkers et al., 2004; Karnath et al., 2004a) demarcated lesions by hand onto standard template images, which limited the precision of border localization (Mort et al., 2003; Karnath et al., 2004b). To overcome this limitation, we used a lesion analysis method that did not rely on subjective transfer of lesions to standard template slices. We masked the lesions and artifacts of the MRI prior to drawing directly on the patient's own MRI scan, then we mapped the scan into a stereotaxic space using an automated normalization process (Brett et al., 2001). Instead of applying the deformation matrix to the lesion shape like Mort et al. (2003), which implies a threshold of the lesion mask due to registration border effects, we drew the ROI on the normalized scan to be sure to respect the border of the lesion.

The voxel-by-voxel statistical analysis raises the same issues of the multiple comparison problem as neuroimaging studies (Rorden and Karnath, 2004). In this kind of study, the number of tests to be conducted is so high that the considerable risk of false positives (claiming a brain region is required for a task when in fact it is not) must be controlled. Thus, the voxel-by-voxel statistical method suffers from the stringent Bonferroni correction applied, resulting in real effects that may not be detected. Our cluster-by-cluster approach greatly reduced the Bonferroni correction by reporting the correction on clusters of voxels instead of individual voxels.

Regarding the localizing power of the cluster-based approach, clusters gather contiguous voxels with exactly the same score values (i.e., clusters which are covered by the same ROIs) and the minimum size of a cluster is a single voxel. In a voxel-based approach, voxels that are part of a same cluster have the same values. When submitted to a statistical test, they all yield the same statistical value, so they behave in fact as a whole cluster of voxels and not as individuals. When applying a correction for multiple comparisons, these voxels either all pass the threshold or are all rejected. It is not possible for some of them to show a different behavior than the others. Thus, there is no difference between the voxel-based approach and AnaCOM in terms of localization. The only difference is that, in the AnaCOM cluster-based approach, the Bonferroni correction for multiple comparisons is less conservative since the test is made on the cluster level and not on the voxel level. This can have different effects. False negatives that would not pass the threshold at the voxel-level may pass the threshold at the cluster level, thus turning true positive, hence improving the sensitivity of the method. Similarly, true negatives that would not pass the threshold at the voxel level might pass the threshold at the cluster level, hence, slightly decreasing the specificity of the method. However, as the finality of this method is to find all the areas of the brain that are necessary to the function tested, a sensitive method is more appropriate than a very specific method. By increasing the sensitivity as compared to voxel-based methods, AnaCOM improves their effectiveness.

Tyler et al. applied a 'VBM like' method in which statistical analysis could rely on clusters. The authors correlated the signal intensity of each voxel of normalized smoothed T1 anatomical MRIs presenting lesions with the score obtained by the patients (Tyler et al., 2005). In their study, the patients had several kinds of lesions (e.g., stroke, tumor excision, herpes encephalitis, semantic dementia). A main objection to the use of this approach was the use of the image intensity as a factor of the ratio lesion/functionality. The different kinds of lesions presented in the study give different intensities, which were not directly relevant to the tissue functionality.

Another statistical approach to the study of lesions exists—the region-based statistical analysis (RBSA) (Committeri et al., 2007). Since its approach is theoretically different than voxel- or cluster-based techniques, we did not make a comparison. This technique

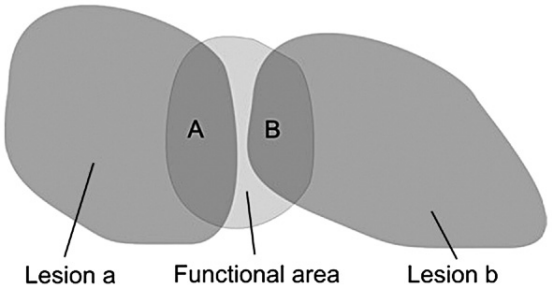

Fig. 11. Hypothesis of lesions partially covering a functional area without touching each other. If the score of the subject having a lesion covering the cluster A was to be compared to the score of the subject covering the cluster B, it would certainly appear similar. If the score of the subject having a lesion covering the cluster A was to be compared to the score obtained by a subject having no lesion, the scores are more likely to be different.

uses a parcellation of the brain. It applies statistics on the volume and the percentage of each brain region damaged. If it were possible to know which part of the regions of the brain are implicated in a functional deficit, it would be interesting to somehow combine it with the AnaCOM method.

Improvement could be made to aspects of the AnaCOM technique such as ROI analysis, and specifically on the statistical aspects (see Fig. 9). Even if comparing clusters instead of voxels greatly reduces the multiple comparisons problem, it is still a concern. Here, we used a Bonferroni correction, a conventional correction method which is very conservative and reduces statistical power. False discovery rate (FDR) correction (Yekutieli and Benjamini, 1999; Benjamini et al., 2001) might provide reasonable statistical power while guarding against false positives (Rorden and Karnath, 2004). FDR will be implemented in a future version of the pipeline.

ANCOVA statistical analysis can also be introduced in the process in order to assess the effects of no interest such as lesion size, age, gender, delay post onset, and so on. Moreover, ANCOVA statistical analysis could help covary out particular clusters of interest (Bates et al., 2003).

Although AnaCOM improves the method of studying lesions in several ways, lesion studies are still limited. Studies relying on lesions have classical limitations. For example, a brain region can be disabled but intact after brain injury, like strokes. To understand healthy brain function, we need to have a good idea of the temporal sequence of information processing. Unfortunately, the lesion methods do not allow us to assess the time course of information processing. Moreover, brain plasticity after damage cannot be taken into account entirely.

Some weaknesses of the lesion study method can be overcome, like differential vulnerability, since some areas of the cortex are particularly likely to be damaged by stroke (Caviness et al., 2002). Therefore, in the case of stroke studies, the locations of lesions are not randomly distributed in the brain (Rorden and Karnath, 2004). In our study, however, the stroke lesion distribution problem was counterbalanced by including other etiologies of brain damage, like resections of glioma.

Another limitation of the AnaCOM method is that it cannot evaluate areas of the brain which are not covered by patients' lesions (see Fig. 11). But, considering that AnaCOM does not require *a priori* selection of either the location of the lesions, nor the value of the score obtained, databases of patients with lesions that cover a larger part of the brain can be imagined. This larger database would increase the number of clusters, thereby decreasing the volume of the clusters, leading to more precise localization of a function, and improvement of statistical analyses.

The lesion-based method also has strengths when compared to PET or functional MRI (fMRI) techniques. It is able to test the role of white matter fibers, while PET and fMRI only show grey matter function; a deficit in the white matter fibers can cause disconnection of two crucial areas for a function. Functional MRI allows one to amass evidence that a particular task correlates with activation in a particular brain area, but it is still not clear if this brain area is necessary to perform this task (Sarter et al., 1996; Karnath et al., 2004b; Rorden and Karnath, 2004). It is even possible that some activated areas have no direct role in information processing. The fMRI technique cannot detect the possible contributions of areas that are constantly active regardless of the task (Rorden and Karnath, 2004). In lesion studies, areas which are shown to be linked to a functional deficit are certainly crucial for the tested function.

Validation study

Our findings provide evidence that specific frontal areas, i.e., the triangular part of the inferior frontal gyrus and the preSMA, are crucial for phonemic fluency task. Decreased verbal fluency has been classically associated with damage to the left prefrontal cortex (Lezak, 1995). A recent meta-analysis focused on verbal fluency in brain-damaged patients also supports the idea that frontal lesions are specifically associated with impairments in phonemic fluency tasks while non-frontal lesions are not (Henry and Crawford, 2004). Specifically, decreased verbal fluency is associated with structures within the frontal lobes: damage to the posterior left inferior frontal gyrus (Broca's area) and the medial frontal region (Krainik et al., 2003; Hillis et al., 2004).

The two above frontal areas are constantly activated in functional imaging studies using verbal fluency tasks (Habib et al., 1996; Phelps et al., 1997; Brannen et al., 2001; Price, 2001; Abrahams et al., 2003; Krainik et al., 2003; Alario et al., 2006). They are part of a large activated network, encompassing the frontal operculum, the inferior frontal gyrus (opercular portion in area 44, triangular portion in area 45 and area 47), the middle frontal gyrus (area 46) and inferior frontal sulcus, the SMA, the preSMA and adjacent cingular cortex, the anterior insula, the mid-dorsal part of the precentral sulcus (area 6, 8, 44) and the posterior superior temporal cortex (Frith et al., 1991; Buckner et al., 1995; Habib et al., 1996; Paulesu et al., 1997; Indefrey and Levelt, 2000; Lehericy et al., 2000; Price, 2001; Abrahams et al., 2003; Frackowiak et al., 2003; Stippich et al., 2003). In our study, clusters of voxels located in these areas in the left hemisphere have been found to contribute to the verbal fluency deficit ($p<0.001$), while the left middle frontal gyrus, the left superior temporal gyrus and all the right-sided regions do not. Activation in the lateral frontal region but not in temporal areas has been found to be a good marker of hemispheric dominance for language, as assessed by the Wada test (Lehericy et al., 2000). The absence of clusters associated with the decreased verbal fluency in the left middle frontal gyrus was surprising, since this area has been found to strongly correlate with the index of hemispheric dominance in the Wada test and has also been found to be reliably and strongly activated in fMRI studies (Lehericy et al., 2000). Our findings suggest that the middle frontal gyrus, although involved in verbal generation, is not critical, i.e., that other brain structures within the neural network for verbal fluency and/or brain plasticity may overcome the functional defect due to the lesion. It is important to note that patients were included in this study several days or months after the onset of the stroke. Therefore, such a compensatory mechanism may not occur in the short term and may explain the importance of the middle frontal gyrus for verbal fluency and language in the Wada test.

In summary, these results highlight the utility of a cluster-by-cluster lesion mapping approach, namely the AnaCOM method, in patients with focal brain damage. Within a given functional brain network, this approach helps to disambiguate areas that are necessary to perform a cognitive task from those that are not critical for the studied cognitive processing. Keeping in mind the advantages of AnaCOM, the present findings indicate that specific left-sided frontal regions contribute to phonemic fluency, while right-sided frontal-temporal regions are not essential for such tasks. Along this line of reasoning, it is of interest to compare results obtained with AnaCOM in the days immediately following the

occurrence of lesions, before plasticity processes can take place, to the results of the present study performed at a chronic stage. Another potential research program, therefore, could be to focus on the impact of the lesions on the surrounding white matter and association fibers, which cannot be assessed by functional imaging studies.

The VSLM study performed in the same conditions as the AnaCOM, on the same data set, with two sample *t*-test performed for each voxel where at least three lesions were present, did not show any voxels with a Bonferroni correction. The difference between the AnaCOM result and the Bonferroni result is due to the number of comparisons. VSLM is a voxel-based approach, thus the correction for multiple comparison was done at a voxel level, involving 349,454 voxels. AnaCOM is a cluster-based approach, thus the multiple comparison process involves only 1642 clusters, which decreases the degree of Bonferroni correction, and increases the statistical power of the analysis and the sensitivity of the test.

Conclusion

We have presented a new method, AnaCOM (Anatomo-Clinical Overlapping Maps), to create anatomo-functional relationships from structural MRI scans of brain-damaged subjects and neuropsychological tests. AnaCOM improves on preceding voxel-based methods in terms of quality of segmentation and statistical power. AnaCOM is also complementary to fMRI and PET imaging, since the strength of one class of method covers the weakness of the other. This method does not require a hypothesis *a priori* for a structure–function correlation, nor does it require selecting patients with similar functional scores. The AnaCOM method permits us to implicate one or more clusters particularly responsible for a neuropsychological deficit. The hypothesis-generating power is what makes this method exceptionally valuable.

References

Abrahams, S., Goldstein, L.H., Simmons, A., Brammer, M.J., Williams, S.C., Giampietro, V.P., Andrew, C.M., Leigh, P.N., 2003. Functional magnetic resonance imaging of verbal fluency and confrontation naming using compressed image acquisition to permit overt responses. Hum. Brain Mapp. 20, 29–40.

Alario, F.X., Chainay, H., Lehericy, S., Cohen, L., 2006. The role of the supplementary motor area (SMA) in word production. Brain Res. 1076, 129–143.

Ashburner, J., Friston, K.J., 1999. Nonlinear spatial normalization using basis functions. Hum. Brain Mapp. 7, 254–266.

Ashburner, J., Neelin, P., Collins, D.L., Evans, A., Friston, K., 1997. Incorporating prior knowledge into image registration [comment]. NeuroImage 6, 344–352.

Ayotte, J., Peretz, I., Rousseau, I., Bard, C., Bojanowski, M., 2000. Patterns of music agnosia associated with middle cerebral artery infarcts. Brain 123, 1926–1938.

Bates, E., Wilson, S.M., Saygin, A.P., Dick, F., Sereno, M.I., Knight, R.T., Dronkers, N.F., 2003. Voxel-based lesion-symptom mapping. Nat. Neurosci. 6, 448–450.

Beblo, T., Wallesch, C.W., Herrmann, M., 1999. The crucial role of frontostriatal circuits for depressive disorders in the postacute stage after stroke. Neuropsychiatry Neuropsychol. Behav. Neurol. 12, 236–246.

Benjamini, Y., Drai, D., Elmer, G., Kafkafi, N., Golani, I., 2001. Controlling the false discovery rate in behavior genetics research. Behav. Brain Res. 125, 279–284.

Bertrand, G., 1994. Simple points, topological numbers and geodesic neighborhoods in cubic grids. Pattern Recogn. Lett. 15, 1003–1010.

Bertrand, G., Malandain, G., 1994. A new characterisation of three dimensional simple points. Pattern Recogn. Lett. 15, 169–175.

Brannen, J.H., Badie, B., Moritz, C.H., Quigley, M., Meyerand, M.E., Haughton, V.M., 2001. Reliability of functional MR imaging with word-generation tasks for mapping Broca's area. AJNR Am. J. Neuroradiol. 22, 1711–1718.

Braun, D., Weber, H., Mergner, T., Schulte-Monting, J., 1992. Saccadic reaction times in patients with frontal and parietal lesions. Brain 115, 1359–1386.

Brett, M., Leff, A.P., Rorden, C., Ashburner, J., 2001. Spatial normalization of brain images with focal lesions using cost function masking. NeuroImage 14, 486–500.

Broca, P., 1861a. Nouvelle observation d'aphémie produite par une lésion de la moitié postérieure des deuxième et troisième circonvolution frontales gauches. Bull. Soc. Anat. 36, 398–407.

Broca, P., 1861b. Perte de la parole, ramollissement chronique et destruction partielle du lobe antérieur gauche. [Sur le siège de la faculté du langage.]. Bull. Soc. Anthropol. 2, 235–238.

Broca, P., 1861c. Remarques sur le siège de la faculté du langage articulé, suivies d'une observation d'aphémie. Bull. Soc. Anat. 36, 330–357.

Broca, P., 1861d. Sur le principe des localisations cérébrales. Bull. Soc. Anthropol. 2, 190–204.

Broca, P., 1863. Localisations des fonctions cérébrales. Siège de la faculté du langage articulé. Bull. Soc. Anthropol. 4, 200–208.

Broca, P., 1865. Du siège de la faculté du langage articulé dans l'hémisphère gauche du cerveau. Bull. Soc. Anthropol. 6, 377–393.

Buckner, R.L., Raichle, M.E., Petersen, S.E., 1995. Dissociation of human prefrontal cortical areas across different speech production tasks and gender groups. J. Neurophysiol. 74, 2163–2173.

Butefisch, C.M., Kleiser, R., Seitz, R.J., 2006. Post-lesional cerebral reorganisation: evidence from functional neuroimaging and transcranial magnetic stimulation. J. Physiol. (Paris) 99, 437–454.

Cardebat, D., Doyon, B., Puel, M., Goulet, P., Joanette, Y., 1990. Formal and semantic lexical evocation in normal subjects. Performance and dynamics of production as a function of sex, age and educational level. Acta Neurol Belg 90, 207–217.

Caviness, V.S., Makris, N., Montinaro, E., Sahin, N.T., Bates, J.F., Schwamm, L., Caplan, D., Kennedy, D.N., 2002. Anatomy of stroke: Part I. An MRI-based topographic and volumetric system of analysis. Stroke 33, 2549–2556.

Clarke, S., Lindemann, A., Maeder, P., Borruat, F.X., Assal, G., 1997. Face recognition and postero-inferior hemispheric lesions. Neuropsychologia 35, 1555–1563.

Cohen, L., Martinaud, O., Lemer, C., Lehericy, S., Samson, Y., Obadia, M., Slachevsky, A., Dehaene, S., 2003. Visual word recognition in the left and right hemispheres: anatomical and functional correlates of peripheral alexias. Cereb. Cortex 13, 1313–1333.

Cointepas, Y., Mangin, J.-F., Garnero, L., Poline, J.-B., Benali, H., 2001. BrainVISA: software platform for visualization and analysis of multi-modality brain data. HBM'2001.

Committeri, G., Pitzalis, S., Galati, G., Patria, F., Pelle, G., Sabatini, U., Castriota-Scanderbeg, A., Piccardi, L., Guariglia, C., Pizzamiglio, L., 2007. Neural bases of personal and extrapersonal neglect in humans. Brain 130, 431–441.

Cromwell, H.C., Berridge, K.C., 1993. Where does damage lead to enhanced food aversion: the ventral pallidum/substantia innominata or lateral hypothalamus? [Erratum appears in Brain Res 1994 Apr 11;642 (1–2):355] Brain Res. 624, 1–10.

Dronkers, N.F., Wilkins, D.P., Van Valin Jr., R.D., Redfern, B.B., Jaeger, J.J., 2004. Lesion analysis of the brain areas involved in language comprehension. Cognition 92, 145–177.

Frackowiak, R., Friston, K., Frith, C.D., Dolan, R., Price, C.J., Zeki, S.,

Ashburner, J., Penny, W., 2003. An overview of speech comprehension and production, Human Brain Function, Second Edition. Elsevier, pp. 517–532.
Frank, R.J., Damasio, H., Grabowski, T.J., 1997. Brainvox: an interactive, multimodal visualization and analysis system for neuroanatomical imaging. NeuroImage 5, 13–30.
Friston, K.J., 1995. Commentary and opinion: II. Statistical parametric mapping: ontology and current issues. J. Cereb. Blood Flow Metab. 15, 361–370.
Frith, C.D., Friston, K., Liddle, P.F., Frackowiak, R.S., 1991. Willed action and the prefrontal cortex in man: a study with PET. Philos. Trans. R. Soc. Lond., B Biol. Sci. 244, 241–246.
Furst, M., Aharonson, V., Levine, R.A., Fullerton, B.C., Tadmor, R., Pratt, H., Polyakov, A., Korczyn, A.D., 2000. Sound lateralization and interaural discrimination. Effects of brainstem infarcts and multiple sclerosis lesions. Hear. Res. 143, 29–42.
Gaymard, B., Rivaud, S., Cassarini, J.F., Dubard, T., Rancurel, G., Agid, Y., Pierrot-Deseilligny, C., 1998. Effects of anterior cingulate cortex lesions on ocular saccades in humans. Exp. Brain Res. 120, 173–183.
Godefroy, O., Duhamel, A., Leclerc, X., Saint Michel, T., Henon, H., Leys, D., 1998. Brain-behaviour relationships. Some models and related statistical procedures for the study of brain-damaged patients. Brain 121 (Pt 8), 1545–1556.
Greenlee, M.W., Smith, A.T., 1997. Detection and discrimination of first- and second-order motion in patients with unilateral brain damage. J. Neurosci. 17, 804–818.
Haaland, K.Y., Harrington, D.L., Knight, R.T., 2000. Neural representations of skilled movement. Brain 123, 2306–2313.
Habib, M., Demonet, J.F., Frackowiak, R., 1996. Cognitive neuroanatomy of language: contribution of functional cerebral imaging. Rev. Neurol. (Paris) 152, 249–260.
Henry, J.D., Crawford, J.R., 2004. A meta-analytic review of verbal fluency performance in patients with traumatic brain injury. Neuropsychology 18, 621–628.
Hillis, A.E., Work, M., Barker, P.B., Jacobs, M.A., Breese, E.L., Maurer, K., 2004. Re-examining the brain regions crucial for orchestrating speech articulation. Brain 127, 1479–1487.
Ihaka, R., Gentleman, R., 1996. R: a language for data analysis and graphics. J. Comput. Graph. Stat. 5, 299–314.
Indefrey, P., Levelt, W., 2000. The neural correlates of language production. In: Gazzaniga, M.S. (Ed.), The New Cognitive Neurosciences. MIT Press, pp. 845–880.
Karnath, H.O., Fruhmann Berger, M., Kuker, W., Rorden, C., 2004a. The anatomy of spatial neglect based on voxelwise statistical analysis: a study of 140 patients. Cereb. Cortex 14, 1164–1172.
Karnath, H.O., Fruhmann Berger, M., Zopf, R., Kuker, W., 2004b. Using SPM normalization for lesion analysis in spatial neglect. Brain 127, E10 (author reply E11).
Kertesz, A., 1993. Clinical forms of aphasia. Acta Neurochir., Suppl. 56, 52–58.
Kinkingnéhun, S.R., du Boisguéheneuc, F., Golmard, J.-L., Zhang, S.X., Levy, R., Dubois, B., 2004. Anatomoclinical overlapping maps (AnaCOM): a new method to create anatomo-functional maps from neuropsychological tests and structural MRI scan of subjects with brain lesions. Medical Imaging'04, San Diego, CA, 14–19 February, pp. 583–592.
Krainik, A., Lehericy, S., Duffau, H., Capelle, L., Chainay, H., Cornu, P., Cohen, L., Boch, A.L., Mangin, J.F., Le Bihan, D., Marsault, C., 2003. Postoperative speech disorder after medial frontal surgery: role of the supplementary motor area. Neurology 60, 587–594.
Leger, A., Demonet, J.F., Ruff, S., Aithamon, B., Touyeras, B., Puel, M., Boulanouar, K., Cardebat, D., 2002. Neural substrates of spoken language rehabilitation in an aphasic patient: an fMRI study. NeuroImage 17, 174–183.
Lehericy, S., Duffau, H., Cornu, P., Capelle, L., Pidoux, B., Carpentier, A., Auliac, S., Clemenceau, S., Sichez, J.P., Bitar, A., Valery, C.A., Van Effenterre, R., Faillot, T., Srour, A., Fohanno, D., Philippon, J., Le Bihan, D., Marsault, C., 2000. Correspondence between functional magnetic resonance imaging somatotopy and individual brain anatomy of the central region: comparison with intraoperative stimulation in patients with brain tumors. J. Neurosurg. 92, 589–598.
Lekwuwa, G.U., Barnes, G.R., 1996. Cerebral control of eye movements: I. The relationship between cerebral lesion sites and smooth pursuit deficits. Brain 119, 473–490.
Lezak, M., 1995. Neuropsychological Assessment. Oxford University Press.
Lippitz, B., Mindus, P., Meyerson, B.A., Kihlstrom, L., Lindquist, C., 1997. Obsessive compulsive disorder and the right hemisphere: topographic analysis of lesions after anterior capsulotomy performed with thermocoagulation. Acta Neurochir., Suppl. 68, 61–63.
Makale, M., Solomon, J., Patronas, N.J., Danek, A., Butman, J.A., Grafman, J., 2002. Quantification of brain lesions using interactive automated software. Behav. Res. Methods Instrum. Comput. 34, 6–18.
Milea, D., Lehericy, S., Rivaud-Pechoux, S., Duffau, H., Lobel, E., Capelle, L., Marsault, C., Berthoz, A., Pierrot-Deseilligny, C., 2003. Antisaccade deficit after anterior cingulate cortex resection. NeuroReport 14, 283–287.
Mort, D.J., Malhotra, P., Mannan, S.K., Rorden, C., Pambakian, A., Kennard, C., Husain, M., 2003. The anatomy of visual neglect. Brain 126, 1986–1997.
Parvizi, J., Damasio, A.R., 2003. Neuroanatomical correlates of brainstem coma. Brain 126, 1524–1536.
Paulesu, E., Goldacre, B., Scifo, P., Cappa, S.F., Gilardi, M.C., Castiglioni, I., Perani, D., Fazio, F., 1997. Functional heterogeneity of left inferior frontal cortex as revealed by fMRI. NeuroReport 8, 2011–2017.
Phelps, E.A., Hyder, F., Blamire, A.M., Shulman, R.G., 1997. FMRI of the prefrontal cortex during overt verbal fluency. NeuroReport 8, 561–565.
Pierrot-Deseilligny, C., Rosa, A., Masmoudi, K., Rivaud, S., Gaymard, B., 1991. Saccade deficits after a unilateral lesion affecting the superior colliculus. J. Neurol. Neurosurg. Psychiatry 54, 1106–1109.
Price, J.B.a.C., 2001. Functional neuroimaging of language. Handbook of Functional Neuroimaging of Cognition. Roberto Cabeza and Alan Kingstone, pp. 187–251.
Regan, D., Giaschi, D., Sharpe, J.A., Hong, X.H., 1992. Visual processing of motion-defined form: selective failure in patients with parietotemporal lesions. J. Neurosci. 12, 2198–2210.
Rivaud, S., Muri, R.M., Gaymard, B., Vermersch, A.I., Pierrot-Deseilligny, C., 1994. Eye movement disorders after frontal eye field lesions in humans. Exp. Brain Res. 102, 110–120.
Rivière, D., Papadopoulos-Orfanos, D., Régis, J., Mangin, J.-F., 2000. A Structural Browser of Brain Anatomy. HBM, San Antonio.
Rorden, C., Karnath, H.O., 2004. Using human brain lesions to infer function: a relic from a past era in the fMRI age? Nat. Rev., Neurosci. 5, 813–819.
Sarter, M., Berntson, G.G., Cacioppo, J.T., 1996. Brain imaging and cognitive neuroscience. Toward strong inference in attributing function to structure. Am. Psychol. 51, 13–21.
Stippich, C., Mohammed, J., Kress, B., Hahnel, S., Gunther, J., Konrad, F., Sartor, K., 2003. Robust localization and lateralization of human language function: an optimized clinical functional magnetic resonance imaging protocol. Neurosci. Lett. 346, 109–113.
Stufflebeam, S.M., Levine, R.A., Gardner, J.C., Fullerton, B.C., Furst, M., Rosen, B.R., 2000. Objective detection and localization of multiple sclerosis lesions on magnetic resonance brainstem images: validation with auditory evoked potentials. J. Basic Clin. Physiol. Pharmacol. 11, 231–258.
Stuss, D.T., Alexander, M.P., Hamer, L., Palumbo, C., Dempster, R., Binns, M., Levine, B., Izukawa, D., 1998. The effects of focal anterior and posterior brain lesions on verbal fluency. J. Int. Neuropsychol. Soc. 4, 265–278.
Tranel, D., Damasio, H., Damasio, A.R., 1997. A neural basis for the retrieval of conceptual knowledge. Neuropsychologia 35, 1319–1327.
Tyler, L.K., Marslen-Wilson, W., Stamatakis, E.A., 2005. Dissociating

neuro-cognitive component processes: voxel-based correlational methodology. Neuropsychologia 43, 771–778.

Van der Werf, Y.D., Scheltens, P., Lindeboom, J., Witter, M.P., Uylings, H.B., Jolles, J., 2003. Deficits of memory, executive functioning and attention following infarction in the thalamus; a study of 22 cases with localised lesions. Neuropsychologia 41, 1330–1344.

Warburton, E., Price, C.J., Swinburn, K., Wise, R.J., 1999. Mechanisms of recovery from aphasia: evidence from positron emission tomography studies. J. Neurol. Neurosurg. Psychiatry 66, 155–161.

Yekutieli, D., Benjamini, Y., 1999. Resampling-based false discovery rate controlling multiple test procedures for correlated test statistics. J. Stat. Plan Infer. 82, 171–196.